Exsolution constructed $FeNi/NiFe_2O_4$ composite: preferentially breaking of octahedral metal-oxygen bonds in spinel oxide

Xiaoyan Guo,[a] Lu Yao,[a] Xiangyan Hou,[a] Xiaofeng Wu,*[a] Yaowen Zhang,[a] Qian Zhu,[a] Zhangtao Guo,[a] Shuting Li,[a] Yilan Jiang,*[b] Keke Huang,*[a] and Shouhua Feng[a]

[a]State Key Laboratory of Inorganic Synthesis and Preparative Chemistry Jilin Provincial International Cooperation Key Laboratory of Advanced Inorganic Solid Functional Materials, College of Chemistry, Jilin University, Qianjin Street 2699, Changchun 130012, China;

[b]Key Laboratory of Integrated Regulation and Resource Development on Shallow Lake of Ministry of Education, College of Environment, Hohai University, Nanjing 210098, China.

E-mail: wuxf@jlu.edu.cn; yljiang21@hhu.edu.cn; kkhuang@jlu.edu.cn.

Table S1. Ni and Fe content of NFO, NFO-400H, NFO-500H and NFO+NF.

Samples	Concentration	
	Ni (ppm)	Fe (ppm)
NFO	55.55	100.9
NFO-400H	52.52	96.48
NFO-500H	60.58	114.4
NFO-600H	79.83	145.5
NFO+NF	64.07	116.4

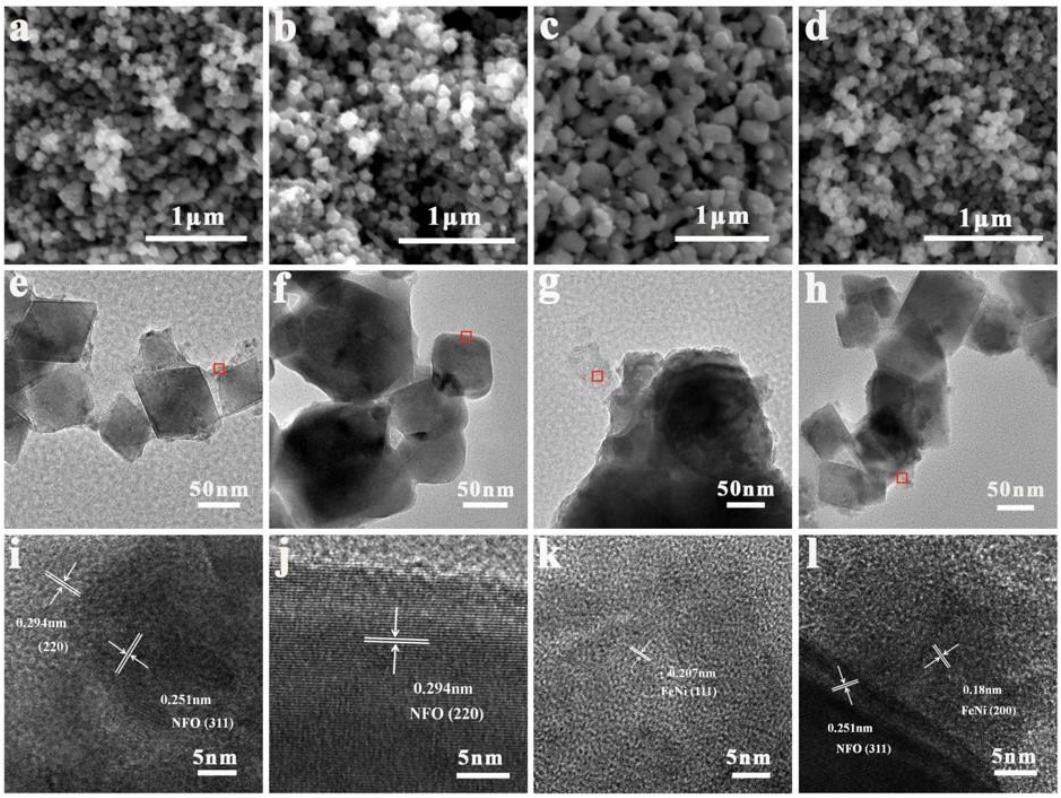

Figure S1. SEM, TEM and HRTEM images of (a, e, i) NFO, (b, f , j) NFO-400H, (c, g, k) NFO-600H, (d, h, l) NFO+NF.

The morphologies of NFO, NFO-400H, NFO-600H and NFO+NF were observed with SEM, TEM and HRTEM images.The lattice fringes of 0.294 nm measured from the HRTEM image are consistent with the (220) crystal plane of the NFO sample. The observed lattice fringes of the NFO-400H sample are the same as the results of NFO. It can be seen from the SEM image that with the increase of annealing temperature, the morphology of the sample changes obviously and the particles agglomerate.

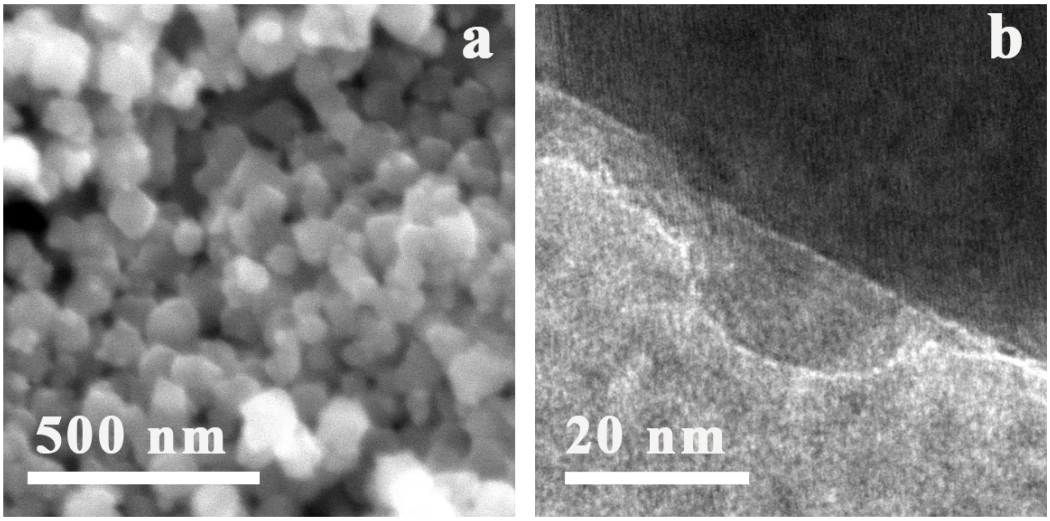

Figure S2. (a) SEM image of NFO-500H. (b) TEM image of NFO-500H.

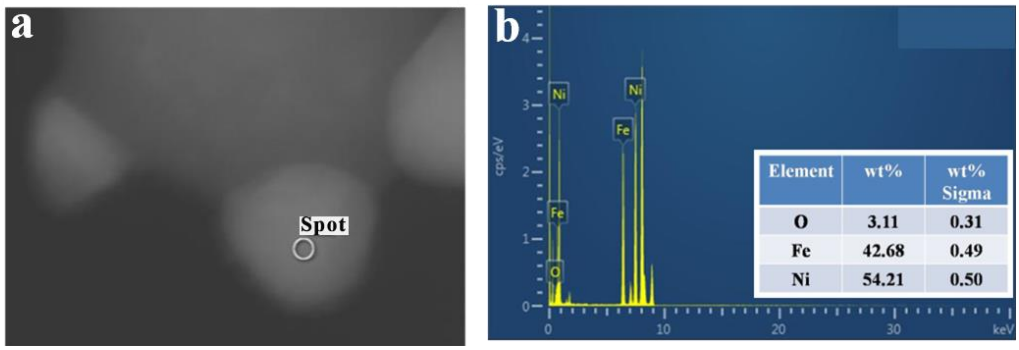

Figure S3. (a-b) HAADF-STEM image of the NFO-500H and the corresponding compositional Spot-scanning results.

Spot-scanning results show that the content of Ni in the exsolved nanoparticles of NFO-500H is relatively higher than that of Fe.

Table S2. O 1s XPS peak deconvolution results and the concentrations of metal ions on surface.

Samples	O_I	O_{II}	Fe^{2+}/Fe^{3+}	Ni^0/Ni
NFO	88.50%	11.50%	43.50%	
NFO-400H	83.33%	16.66%	50.25%	
NFO-500H	79.36%	20.63%	52.63%	19.01%
NFO-600H	67.57%	32.43%	60.97%	27.65%

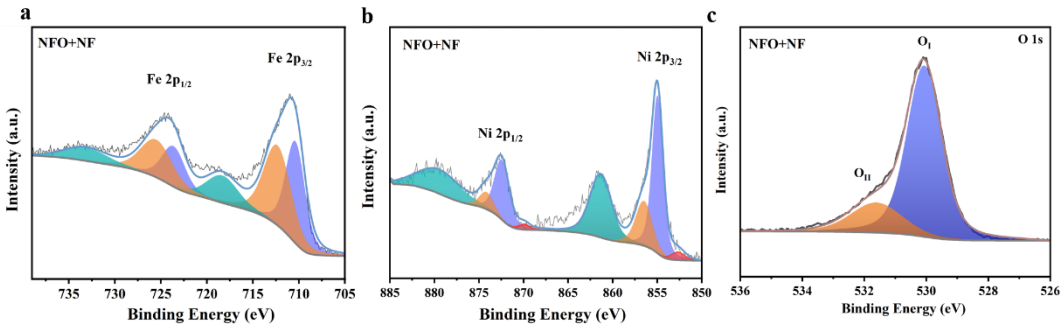

Figure S4. XPS spectra of (a) Fe 2p, (b) Ni 2p and (c) O 1s of NFO+NF.

Table S3. Detailed of O K-edge and Fe L-edge XANES of NFO, NFO-400H, NFO-500H and NFO-600H.

	NFO	NFO-400H	NFO-500H	NFO-600H
Ratio of I_B/ I_A	1.38	0.92	0.95	0.938
Energy (eV): Fe t_{2g} (A)	709.7	709.8	709.8	709.6
Energy (eV): Fe e_g (B)	711.06	711.03	710.99	710.86
Fe $\Delta E(t_{2g}\text{-}e_g)$ (eV)	1.37	1.23	1.19	1.26

Table S4. Mössbauer parameters for NFO, NFO-400H, NFO-500H and NFO-600H.

Samples	Component	IS (mm/s)	QS (mm/s)	Magnetic field (T)	Area Ratio (%)
NFO	I	0.359	0.014	51.29	49.87
	II	0.258	0.011	48.17	50.13
NFO-400H	I	0.362	0.015	52.04	49.27
	II	0.251	0.021	48.69	50.73
NFO-500H	I	0.374	-0.066	52.32	17.59
	II	0.265	0.029	48.99	43.17
	III	0.751	0.082	47.71	21.5
	IV	0.003	0	30.45	17.73
NFO-600H	IV	-0.011	0	14.34	52.03
	IV	0.014	0	26.51	47.97
NFO+NF	I	0.399	0.015	50.69	32.27
	II	0.220	-0.07	48.65	32
	IV	-0.021	0	21.6	35.73

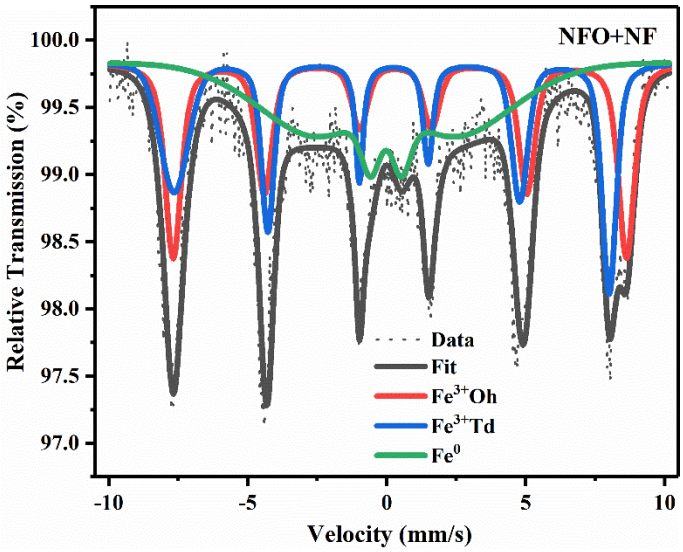

Figure S5. Mössbauer spectra of NFO+NF.

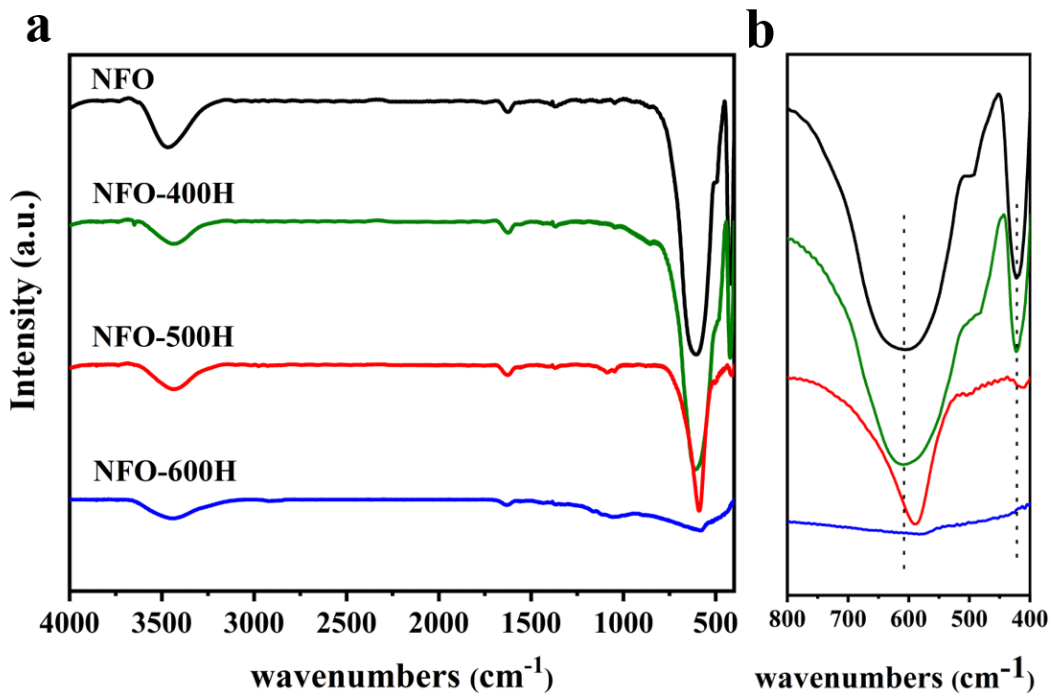

Figure S6. (a) FT-IR (b) Enlarged IR patterns at 800-400 wavenumbers of (a).

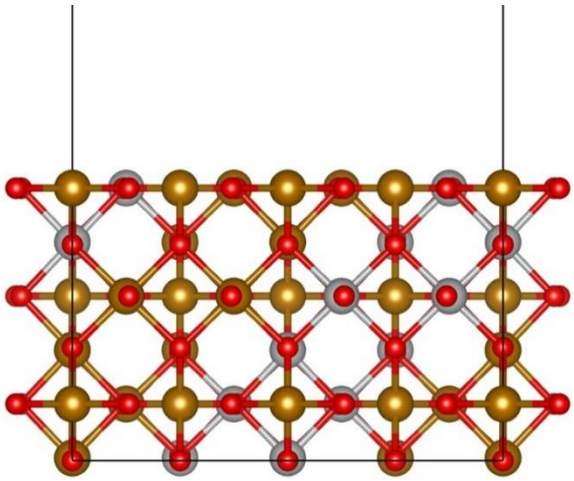

Figure S7. (110) slab model of $NiFe_2O_4$.

Calculation detail of bond energy and segregation energy

1. The calculation of bond energy:

$$E_{bond} = (E_{bulk\_M\_defect} + E_M - E_{bulk}) / n$$

2. The calculation of the segregation energy:

$$E_{seg} = E_{after} - E_{before}$$

Table S5. The OER activity of some spinel catalysts in alkaline media.

Catalysts	Electrolyte	Overpotential@10 mA cm^{-2} (mV)	Reference literature
NFO-500H	1 M KOH	283	This work
$NiCrFeO_4$	1 M KOH	298	[1]
$NiCo_{2-x}Fe_xO_4$ NBs	1 M KOH	274	[2]
Ni_3S_2@FeNi-$NiFe_2O_4$/C	1 M KOH	280	[3]
FeNi/$NiFe_2O_4$@NC	1 M KOH	316	[4]
OP-$NiFe_2O_4$/NCNF	1 M KOH	260	[5]
NiO/$NiFe_2O_4$ nanosheets	1 M KOH	279	[6]
$(Co_{0.2}Mn_{0.2}Ni_{0.2}Fe_{0.2}Zn_{0.2})Fe_2O_4$	1 M KOH	326	[7]
Ni/$NiFe_2O_4$-CNTs	1 M KOH	311	[8]

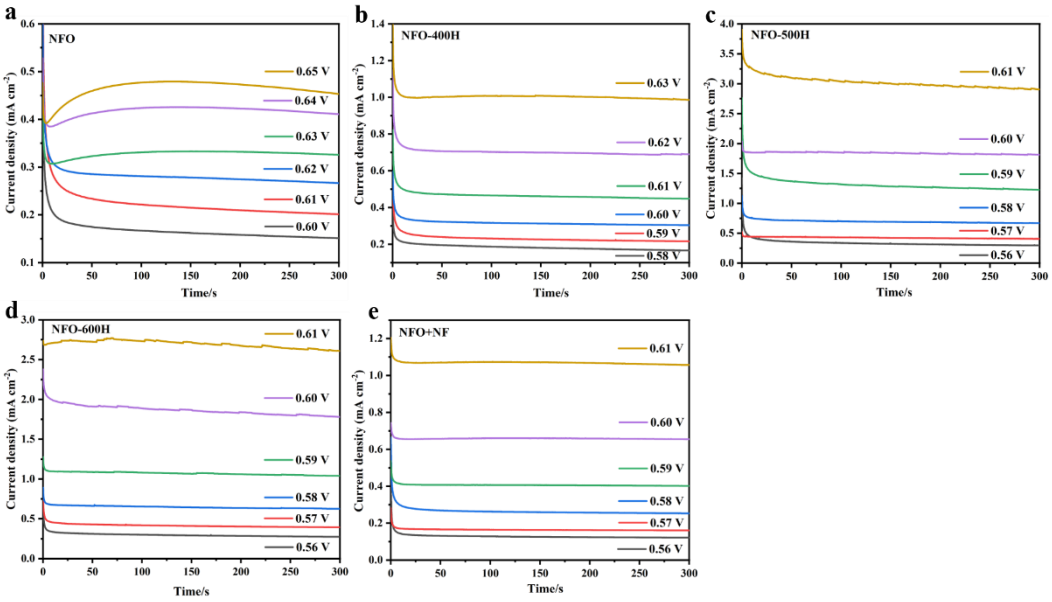

Figure S8. Multipotential step of (a) NFO, (b) NFO-400H, (c) NFO-500H, (d) NFO-600H and (e) MFO+NF was used to acquire the Tafel slope of samples. The time required to reach the steady state was 5 min.

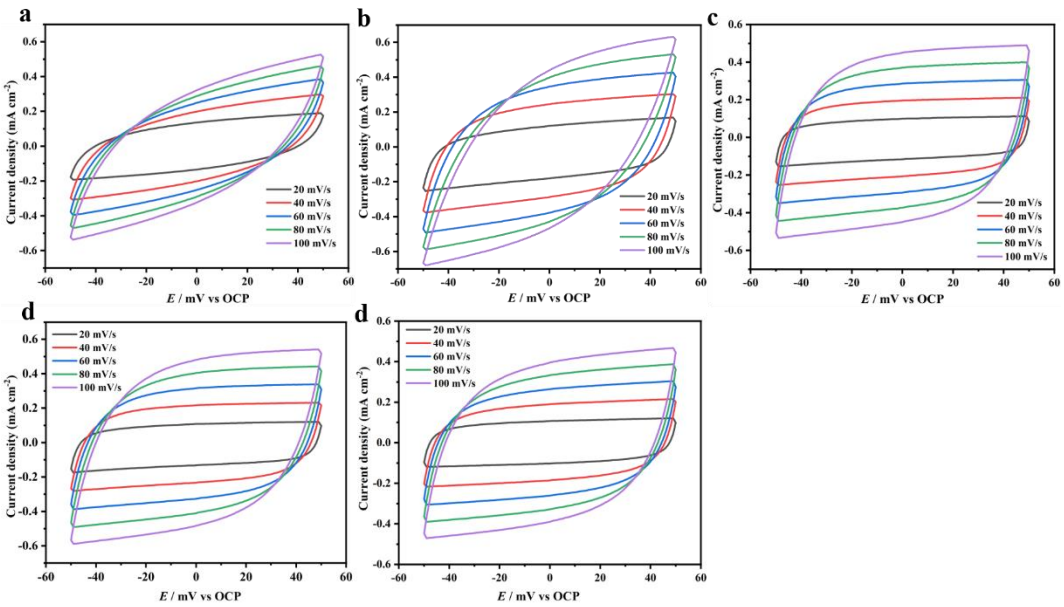

Figure S9. CV measurements at different scan rates of (a) NFO, (b) NFO-400H, (c) NFO-500H, (d) NFO-600H and (e) NFO+NF.

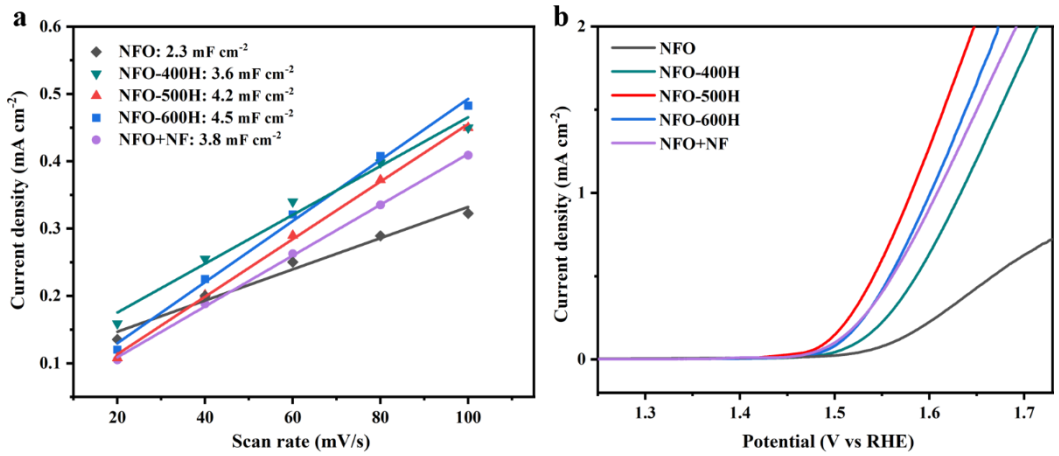

Figure S10. (a) C_{dl} plotted from scan rates of NFO and reduced NFO composites. (b) LSV curves of catalysts using ECSA normalized current density.

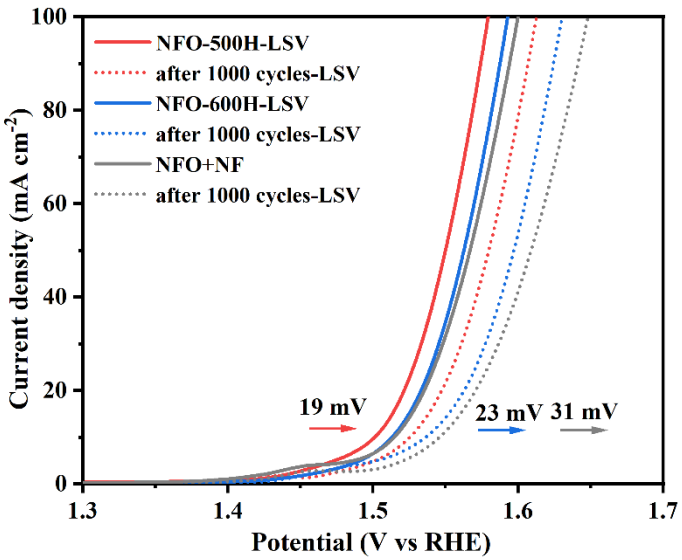

Figure S11. LSV before and after 1000 CV cycles for OER of NFO-500H, NFO-600H and NFO+NF.

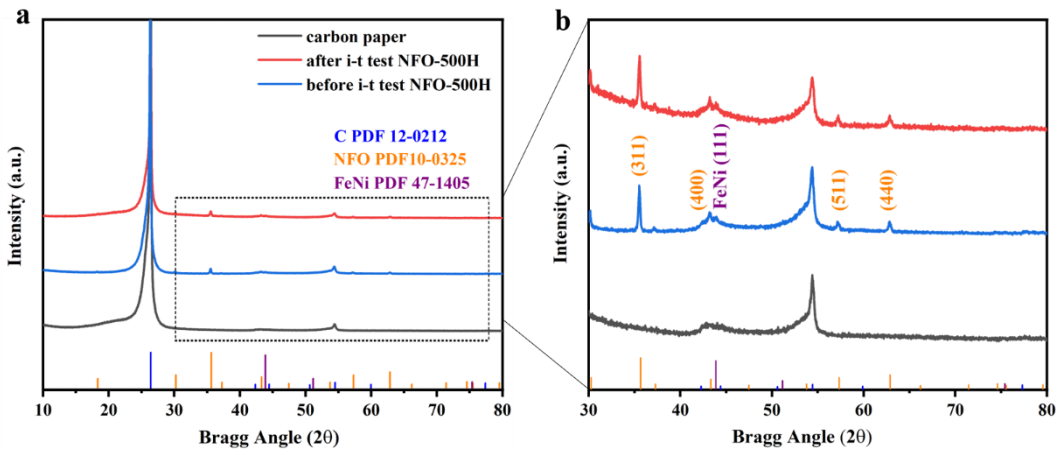

Figure S12. (a) XRD pattern of NFO-500H before and after long-term stability measurement. (b) Enlarged XRD patterns at 30°-80°of (a).

The stability test of NFO-500H was carried out on carbon paper and the structure after tested was characterized by XRD. The XRD results show that the NFO-500H phase remains after the electrochemical stability test, and the FeNi alloy peak still exists.

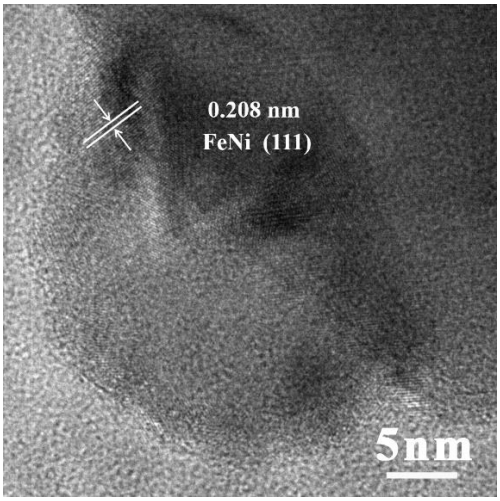

Figure S13. HRTEM images of the NFO-500H after LSV curves.

Notes and references

1. P. Ramakrishnan, K. B. Lee, G.-J. Choi, I.-K. Park and J. I. Sohn, *Ind. Eng. Chem. Res.*, 2021, **101**, 178-185.
2. Y. Huang, S. L. Zhang, X. F. Lu, Z. P. Wu, D. Luan and X. W. D. Lou, *Angew. Chem. Int. Ed.*, 2021, **60**, 11841-11846.
3. L. Xu, S. Ali Shah, H. Khan, R. Sayyar, X. Shen, I. Khan, A. Yuan, W. Yaseen, Z. Ali Ghazi, A. Naeem, H. Ullah, X. Li and C. Wang, *J. Colloid Interface Sci.*, 2022, **617**, 1-10.
4. Y. Ma, X. Dai, M. Liu, J. Yong, H. Qiao, A. Jin, Z. Li, X. Huang, H. Wang and X. Zhang, *ACS Appl. Mater. Interfaces.*, 2016, **8**, 34396-34404.
5. W. Zong, D. Rao, H. Guo, Y. Ouyang, Y. E. Miao, W. Wang, J. Wang, F. Lai and T. Liu, *Nanoscale*, 2020, **12**, 10977-10986.
6. H. Zhong, G. Gao, X. Wang, H. Wu, S. Shen, W. Zuo, G. Cai, G. Wei, Y. Shi, D. Fu, C. Jiang, L. W. Wang and F. Ren, *Small*, 2021, **17**, 2103501.
7. Y. Zhang, T. Lu, Y. Ye, W. Dai, Y. a. Zhu and Y. Pan, *ACS Appl. Mater. Interfaces.*, 2020, **12**, 32548-32555.
8. X. Yu, G. Chen, Y. Wang, J. Liu, K. Pei, Y. Zhao, W. You, L. Wang, J. Zhang, L. Xing, J. Ding, G. Ding, M. Wang and R. Che, *Nano Research*, 2020, **13**, 437-446.